



## 1 INTRODUCTION

Model calibration methods improve the correlation between finite element models (FEM) and measured data. The aim is to obtain the most predictive analytical model despite their incompleteness to describe exactly the underlying physics: most of the parameters should be considered as uncertain rather than nominal values due to manufacturing and experimental variability. In this case, a stochastic calibration method should be use.

On the other hand, the calibration convergence can be wrong due to physical compensating effects which lead to fidelity-equivalent solutions. The info-gap theory provides a way to ensure that the system remains reliable even under these unknown compensating effects. This paper presents an approach to enhance the robustness of a stochastic calibration method using the info-gap theory.

## 2 ROBUST CALIBRATION

### 2.1 Calibration performances

We wish to compare experimental data results to simulated outputs. A common metric to evaluate deterministic calibration performances is the normed Euclidean distance  $D_E$ :

$$D_E = \sum_{i=1}^n \frac{\sqrt{(v_{a_i} - v_{m_i})^2}}{v_{m_i}} \quad (1)$$

$v_m$  is a vector containing the nominal eigenfrequencies measured ( $n$  outputs) and  $v_a$  the corresponding vector containing the nominal analytical responses and the same number of outputs.

Parameters may be considered as uncertain and defined by probability density functions. In this case, the model now provides uncertain outputs and can be calibrated using stochastic approaches such as covariance adjustment [? ], Gibbs sampling [? ] and Metropolis-Hasting algorithm [? ]. The Euclidean distance is not suitable to compare two unknown distributions whereas Bhattacharya distance  $D_B$  is relevant to evaluate multivariate features [? ]. This metric takes into account both the mean-difference and the covariance difference between the two distributions :

$$D_B = \frac{1}{8}(\bar{v}_a - \bar{v}_m)^T \Sigma^{-1}(\bar{v}_a - \bar{v}_m) + \frac{1}{2} \ln\left(\frac{\det(\Sigma)}{\sqrt{\det \Sigma_a \det \Sigma_m}}\right) \quad (2)$$

with  $\bar{v}_m$  the vector containing the measured eigenfrequencies mean values and  $\bar{v}_a$  the mean vector of the mean analytical responses. The pooled matrix  $\Sigma$  is given by the combination of  $\Sigma_m$  the covariance of the experimental eigenfrequencies and  $\Sigma_a$  the covariance of the analytical outputs as  $\Sigma = \frac{\Sigma_a + \Sigma_m}{2}$ .

### 2.2 Info-gap theory

Info-gap theory has its origins in Ben-Haim [2] studying the reliability of mechanical systems. Since, this approach has been use on a wide range of applications such as climate models [3] and medical researches [4]. The purpose of info-gap is to provide tools for decision-makers in order to assess risks and opportunities of a model in light of the analysis of severe lack of information.

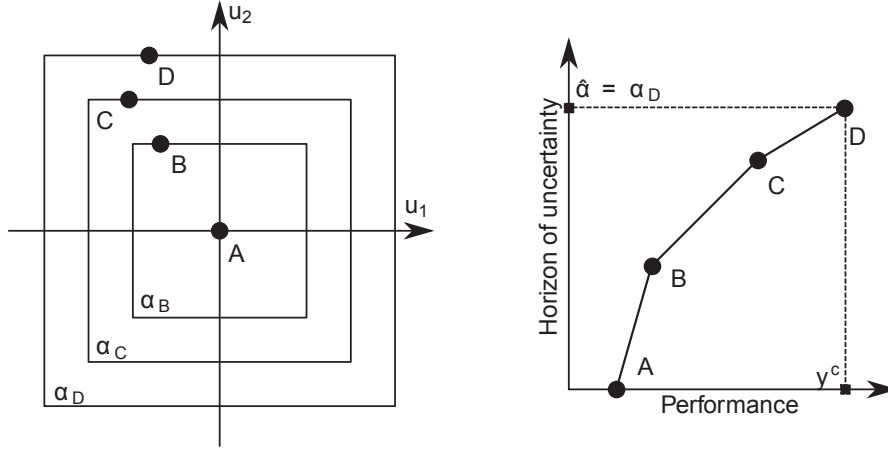


Figure 1. Nested subsets (left) - Robustness curve (right).

In practice, important modeling information may be lacking due to an incomplete understanding of the underlying physics. Hence, probability density functions are not generally suitable alone to describe severely uncertain parameters  $\theta$ .

We introduce the horizon of uncertainty characterized by  $\alpha$ . The larger  $\alpha$ , the greater the range of unknown parameter variations i.e. a bigger space is available for uncertain parameters. Numerical model performances are commonly defined by a function which assess the quality of the response fidelity. Consequently, a catastrophic failure may appear for one set of uncertain parameters sampled from the previous space.

Let's consider several horizons of uncertainty  $\alpha_i$ , the function that yields the worst case model predictions for a given horizon  $\alpha$  is called  $\hat{R}$  and calculated as follow [5] :

$$\hat{R}(\alpha) = \max_{\theta \in U(\alpha, \tilde{\theta})} R(\theta) \tag{3}$$

$\tilde{\theta}$  is the calibrated best-estimate parameter values of the simulation model. The robustness function expresses the greatest level of uncertainty at which performance remains acceptable.

$$\hat{\alpha} = \max\{\alpha : \hat{R}(\alpha) \geq R_c\} \tag{4}$$

with  $\hat{\alpha}$  the maximum horizon to which info-gap uncertainty model is allowed to expand as long as minimal requirements  $R_c$  are satisfied.

The figure 1 explains in a schematic way the method to compute robustness curve [6]. The unknown parameters are  $u_1$  and  $u_2$ . At the first step  $\alpha_A$ , we consider no uncertainty thus the space contains a single point A which is necessarily the worst case. The respective performance  $R(u_{1A}, u_{2A})$  is noted on the robustness curve on the right. Second step, the horizon of uncertainty is increased to  $\alpha_B$ . In the space defined by  $\alpha_B$ , the worst case can be found using a factorial design or by optimization [7]. The algorithm returns the worst case B and report it on the robustness curve. The procedure can be repeated for as much nested subsets required.

### 3 NUMERICAL APPLICATION

A new generation of ceramic matrix composite (CMC) turbine blades have been developed [8]. These materials show high resistance to extremely high temperature (1000°C), low density and a good fracture toughness compared to conventional metallic alloys.

The approach developed previously is applied to a CMC plate perfectly clamped with a progressively reducing thickness. The plate is itself divided into three isotropic material parts to represent physical heterogeneity due to the industrial process. Differences between the experimental results and the numerical outputs will be analyzed through the first three eigenfrequencies of the structure.

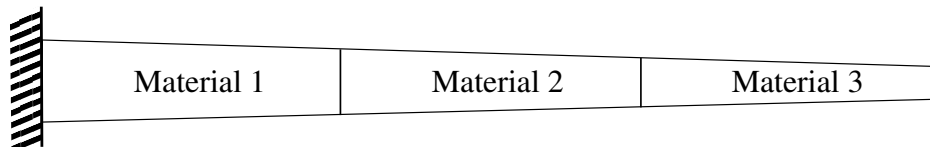


Figure 2. Material properties distribution.

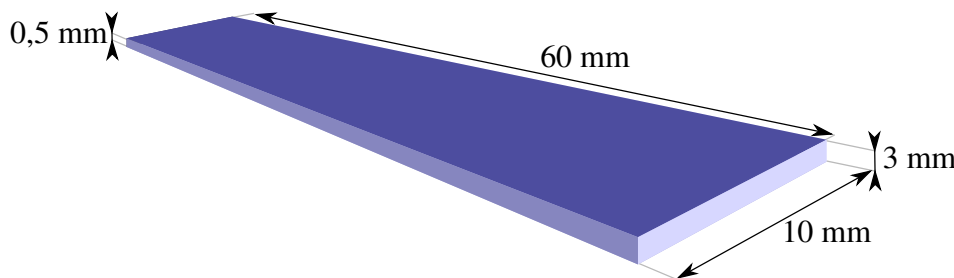


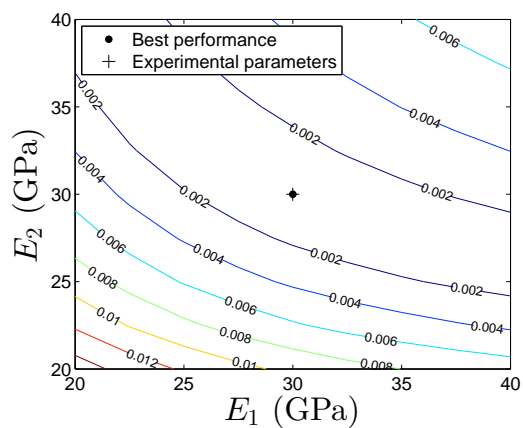
Figure 3. Plate dimensions.

The system is studied through material 1 and material 2 Young's Modulus, noted respectively  $E_1$  and  $E_2$ . The range of parameters  $E_1$  and  $E_2$  values is [20 GPa;40 GPa], divided into a  $20 \times 20$  grid. Thus, 300 Monte-Carlo sampling are achieved with NASTRAN for each combination of parameters using these values as mean. The parameters variance are defined as 10% of the corresponding mean values.

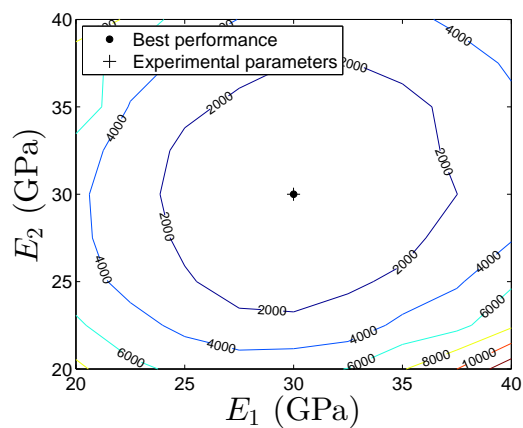
For the simulated test data, 500 experiments are sampled in the same way with  $E_1 = E_2 = 30$  GPa and their variances  $\sigma_{E_1} = \sigma_{E_2} = 3$  GPa. No model form error is added between the two samples. The nominal exact outputs are  $\nu_1 = 18.15$  Hz,  $\nu_2 = 50.64$  Hz and  $\nu_3 = 78.25$  Hz.

The error surface responses are plotted in the space of the two parameters (Figure 4). The contours illustrate fidelity-equivalent solutions and define satisfying boundaries. The best performance marker stands for the global minimal distance found in the discrete space. As expected, this marker totally coincides with the experimental parameters marker for both distance metrics. In this case, the corresponding couple of parameters provides exact and optimal solutions.

In Figure 4(a), there is a slender space where the error remains below 0.2%. It means that deterministic calibrating algorithms can find acceptable set of parameters quite far from the actual experimental parameters. These compensating effects are inevitable even in the absence of bias in the model prediction. In Figure 4(b), the isocontours create nested circles which the lowest error is located in the center. In this case, stochastic calibration should provide relevant updated parameters.



(a) Euclidean isocontour.



(b) Bhattacharya isocontour.

Figure 4. Euclidean and Mahalanobis distances.

## 4 CONCLUSION

This paper proposes a framework to motivate the robust calibration process. In the case study, material parameters have been considered uncertain and the compensating effects between them as a lack of knowledge. Successful updating provides parameters which minimize the error between simulated experiments and analytical outputs while taking into account unavoidable compensating effects. Two calibration metrics have been investigated, in particular a deterministic euclidean error as well as the statistical Bhattacharyya error.

## REFERENCES

- [1] Y. Govers and M. Link. Stochastic model updating - Covariance matrix adjustment from uncertain experimental modal data. *Mechanical Systems and Signal Processing*, 24(3):696–706, April 2010.
- [2] Yakov Ben-Haim. *Info-gap decision theory: decisions under severe uncertainty*. Academic Press, 2006.
- [3] Jim W. Hall, Robert J. Lempert, Klaus Keller, Andrew Hackbarth, Christophe Mijere, and David J. McInerney. Robust Climate Policies Under Uncertainty: A Comparison of Robust Decision Making and Info-Gap Methods: **A Comparison of Robust Decision Making and Info-Gap Methods**. *Risk Analysis*, 32(10):1657–1672, October 2012.
- [4] Y. Ben-Haim, M. Zacksenhouse, C. Keren, and C.C. Dacso. Do we know how to set decision thresholds for diabetes? *Medical Hypotheses*, 73(2):189–193, August 2009.
- [5] Sez Atamturktur, Zhifeng Liu, Scott Cogan, and Hsein Juang. Calibration of imprecise and inaccurate numerical models considering fidelity and robustness: a multi-objective optimization-based approach. *Structural and Multidisciplinary Optimization*, August 2014.
- [6] Emmanuel Pillet. *Méthodologies d'aide à la décision en conception robuste*. PhD thesis, Université de Franche-Comté, 2008.
- [7] Antoine Kuczkowiak. *Modèle hybride incertain pour le calcul de réponse en fonctionnement d'un alternateur*. PhD thesis, Université de Franche-Comté, 2014.
- [8] SNECMA and HERAKLES. Aube de Turbomachine en Matériau Composite et Procédé pour sa Fabrication - Brevet. *WO 2011/080443 A1*, July 2011.

## COPYRIGHT NOTICE

Copyright ©2015 by the authors. Distribution of all material contained in this paper is permitted under the terms of the Creative Commons license Attribution-NonCommercial-NoDerivatives 4.0 International (CC-by-nc-nd 4.0).

